The American Journal of Human Genetics, Volume *104*

Supplemental Data

Heterozygous *RNF13* Gain-of-Function Variants Are Associated with Congenital Microcephaly, Epileptic Encephalopathy, Blindness, and Failure to Thrive

Simon Edvardson, Claudia M. Nicolae, Grace J. Noh, Jennifer E. Burton, Giuseppe Punzi, Avraham Shaag, Jessica Bischetsrieder, Anna De Grassi, Ciro Leonardo Pierri, Orly Elpeleg, and George-Lucian Moldovan

SUPPLEMENTAL DATA

Supplemental Note: Case Report

The affected individual (affected individual 1 in table 1) was a 20 month old male, second of two children to healthy, nonconsanginous parents.

During pregnancy, elevated Alpha-Feto-Protein was noted and from the 22nd week of pregnancy head circumference was discordant with gestational age averaging one week behind the expected. Amniocentesis was declined. Delivery was uneventful at term with a birth weight of 2850 grams, and a head circumference of 31.5 cm that rose to 33 cm by two weeks of age. Within two days after birth irritability, increased appendicular tone and feeding difficulties were noted. No psychomotor development was noted from birth. No eye-contact or voluntary movement were recorded. At age 7 weeks epilepsy presented with refractory, generalized, nonfebrile, Status Epilepticus that persisted for several hours despite treatment with Benzodiazepines, Barbiturates, and Levetiracetam. Subsequent seizures were myoclonic, and generalized Tonic-Clonic. EEG was abnormal with a slow, disorganized background and multifocal interictal spikes. Treatment with Vigabatrin was not effective and Ketogenic diet was partially effective.

Cortical Visual Impairment was diagnosed by few months of age and sensorineural deafness led to cochlear implants by one year of age. No evidence of hearing was obtained subsequently. Persistent feeding difficulties and poor weight gain led to insertion of a Gastrostomy tube.
At the time of initial examination in our clinic (age 20 months) weight was 7.3 kg, height: 76 cm, and head circumference was 40.3 cm. No tracking, response to noise or touch was elicited. Roving eye-movements were noted. The boy was noted to have adducted thumbs (as did his father) and no other dysmorphic or neurocutaneous stigmata. Spasticity was noted in both upper and lower extremities while truncal tone was reduced. No hyperreflexia or upgoing Babinsky's sign was noted. Contractures of lower limbs were present in hamstrings and plantar flexors. Pupils were reactive to light, tongue was in midline and no facial asymmetry was noted. No extrapyramidal movements were noted and the rest of the examination was unremarkable.

Metabolic workup including blood lactate, ammonia, very long chain fatty acids, amino acids, biotinidase activity, isoelectrofocusing of transferrins and acylcarnitine levels were normal as were CSF amino acids and glucose. Brain MRI at age 3 months revealed a thin Corpus Callosum. At 33 months the boy was admitted to hospital with a suspected sepsis that led to his death. No pathogenic agent was identified and autopsy was declined.

Supplemental Figures

Modification Sites in Parent Protein, Orthologs, and Isoforms

Show Multiple Sequence Alignment

LTP	HTP	human		mouse	
0	1	K141	SNDIEVLKKIDIPSV	K141-ub	SNDIDTLkKIDIPSV
0	31	K233-ub	LPVHKFKkGDEYDVC	K233-ub	LPVHKFKkGDEYDVC
0	1	T272	KCVDPWLTkTkKTCP	T272-p	KCVDPWLtkTKKTCP
0	28	K273-ub	CVDPWLTkTkKTCPV	K273-ub	CVDPWLtkTKKTCPV
0	6	K275-ub	DPWLTkTkKTCPVCK	K275	DPWLtkTKKTCPVCK
0	1	S292	VVPSQGDSDSDTDSS	S292-p	VVPSQGDsDsDtDss
0	1	S294	PSQGDSDSDTDSSQE	S294-p	PSQGDsDsDtDssQE
0	1	T296	QGDSDSDTDSSQEEN	T296-p	QGDsDsDtDssQEEN
0	1	S298	DSDSDTDSSQEENEV	S298-p	DsDsDtDssQEENQV
0	1	S299	SDSDTDSSQEENEVT	S299-p	sDsDtDssQEENQVS
0	1	T309-p	ENEVTEHtPLLRPLA	T309	ENQVSEHTPLLPPSA
0	1	S319-p	LRPLASVsAQSFGAL	R319	LPPSASARTQSFGSL
0	2	T380-p	RDYNIANtV_____	T380	QDYNIANTV_____

Figure S1. List of RNF13 experimentally observed PTMs retrievable on phosphositePlus (see Web Resources in the Main Text).

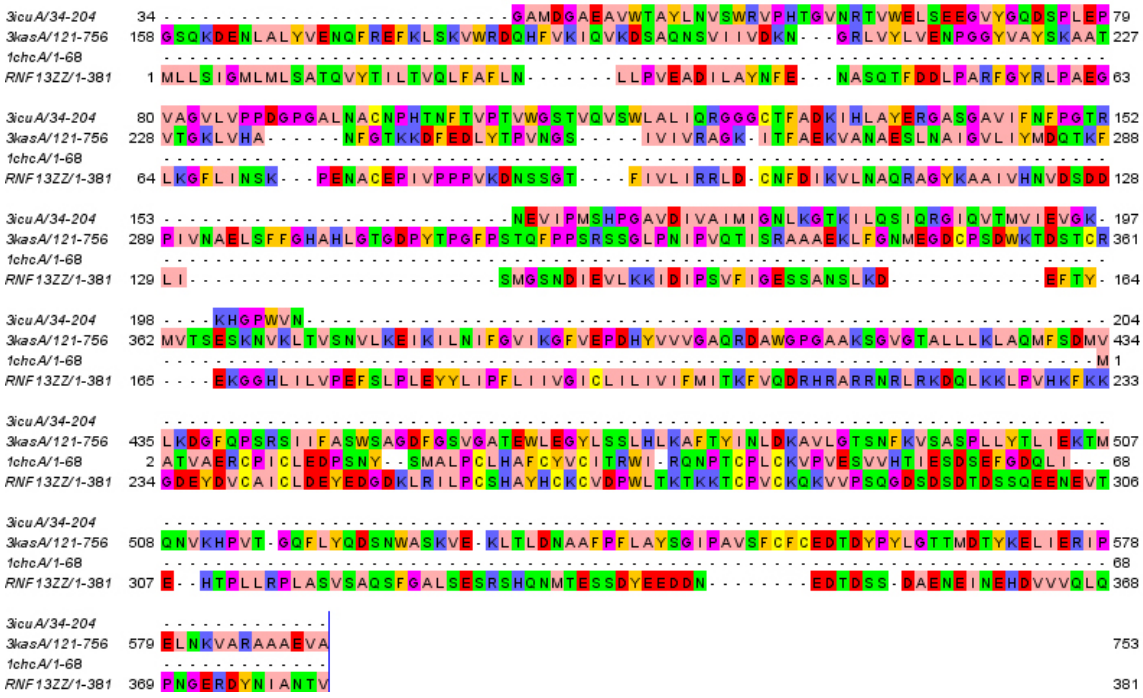

Figure S2. The sequence structure alignment between RNF13 and the sequences of the crystallized structures 3icu.pdb, 3kas.pdb and 1chc.pdb, reported according to pGenThreader and pDomThreader predictions. The alignment figure was generated by using Jalview and the color zappo-style.

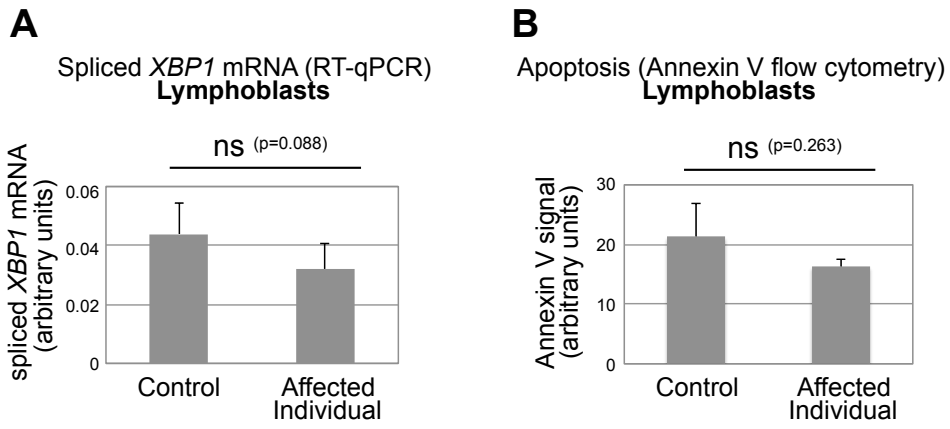

Figure S3. Baseline *XBP1* splicing and apoptosis levels are not significantly different in the affected individual's cells.

(A) Quantification of spliced *XBP1* mRNA by RT-qPCR under baseline (no drug treatment) conditions (non-normalized data). The average of 6 experiments, with standard deviations indicated as error bars, is shown. Statistical significance (TTEST, two-tailed, unequal variance) is indicated.

(B) Quantification of baseline (no drug treatment) apoptosis levels (non-normalized data). The average of 3 experiments, with standard deviations indicated as error bars, is shown. Statistical significance (TTEST, two-tailed, unequal variance) is indicated.

Materials and methods

Cell studies: Fibroblasts and lymphoblasts cells were grown in RPMI media supplemented with 10% FBS. For gene knockdown, cells were transfected with Stealth siRNA (Life Tech) using Lipofectamine RNAiMAX reagent. The RNF13 siRNA oligonucleotide sequence used was: GCCACCUUAUCUUAGUUCCAGAAUU. Cell lysates were obtained by incubating cells in lysis buffer (4% SDS, 2M β-mercaptoethanol, 0.1M Tris pH 6.8) for 15 minutes at 95°C. Antibodies used for Western blots are: RNF13 (Novus NBP1-31251); GAPDH (Santa Cruz Biotechnology sc-47724); IRE1 (Santa Cruz Biotechnology sc-390960); spliced XBP1 (Cell Signaling Technology 12782); phospho-Jun Ser73 (Cell Signaling Technology 3270); Vinculin (Santa Cruz Biotechnology sc-73614). Cellular apoptosis was quantified using the FITC Annexin V kit (Biolegend 640906) according to the manufacturer's instructions. FITC fluorescence intensity was measured using a BD FACSCanto flow cytometer.

RT-qPCR: Total mRNA was purified using TRIzol reagent (Invitrogen), and subjected to reverse transcription using the RevertAid Reverse Transcriptase Kit (Thermo Fisher Scientific) with oligo dT primers. Real-time qPCR was performed with PerfeCTa SYBR Green SuperMix (Quanta), using a CFX Connect Real-Time Cycler (BioRad). The cDNA of *GAPDH* gene was obtained and analyzed in parallel for normalization. Primers used were: spliced *XBP1* (from [1]) (for: TGCTGAGTCCGCAGCAGGTG; rev: GCTGGCAGGCTCTGGGGAAG); and *GAPDH* (for: TGCACCACCAACTGCTTAGC; rev: GGCATGGACTGTGGTCATGAG).

***Sequence analysis*:** RNF13 orthologs were sampled from metazoan by using blastp.

Comparative modeling analysis: Crystal structures of the RNF13 or close paralogs are not available. Thus, related structures for comparative andalysis and 3D modeling were sampled by using pGenThreader, pDomThreader and Modeller tools (see [2] and references therein). The retrieved sequences, including the proposed template structures to be used for comparative modeling, were aligned by using ClustalW (see [2] and references therein). The sequence-structure alignment was used for generating a 3D multi-template model of the human wild type RNF13 protein according to Modeller protocols ([3], see [2] and references therein). 3D models of

the RNF13_Leu311Ser and of the RNF13_Leu312Pro mutants were built by using the in silico mutagenesis tools of PyMOL. A slow molecular dynamics simulation with an annealing procedure[4] was repeated to generate 100 optimized RNF13 wild type and mutant models, according to our validated protocols[2]. The structural properties of the RNF13 wild type and mutant 3D models with the best energy function were evaluated using the biochemical/computational tools of the WHAT IF Web server (http://swift.cmbi.ru.nl/servers/html/index.html). Final models were examined in PyMOL (http://www. pymol.org/) and SwissPDBViewer (http://spdbv.vital-it.ch/).

Generation of a 3D model for RNF13. The RNF13 model was produced by performing multi-template comparative modeling using the crystallized structures of 1chc.pdb[5]; 3icu.pdb (http://www.rcsb.org/pdb/explore/explore.do?structureId=3icu) and 3kas.pdb[6], according to pGenThreader and pDomThreader[7]. Modeller software[8] was used for generating the 3D model using the above cited multi-template sequence structure alignment (Figure S2). The generated model (Figure 2) shows the PA_C_RZF, like domain located at the N-terminal of RNF13 (at the level of RNF13 residues 23-180). In particular, RNF13 residues Phe55-Ile171 (out of 381) are modelled on residues Tyr71-Asn204 of 3icu.pdb and on residues Tyr219-Leu372 of the chainA of 3kas.pdb (out of 760 residues) (Figure S2). Moreover, the model shows the RING_H2_RNF167 domain, rich in Cys and His residues, possibly involved in the binding of Zn located at the C-terminal of RNF13 (at the level of residues 238-283). Notably, the ring domain overlaps with the APC11 domain (at the level of residues 238-291) possibly involved in posttranslational modification, protein turnover, chaperones / Cell division and chromosome partitioning. In particular, RNF13 residues Lys233-Asn303 are modeled on the 68 residues of 1chc.pdb (Figure 2). At the end of the C-terminal domain, a putative PEST and a serine rich sequence motifs can be observed (Figure 2). pGenThreader, pDomThreader and other similar template predictors did not suggest good templates for the modeling of this region. Nevertheless, the RNF13 region including residues Glu304-Val381 shares with the 3kas c-terminal domain (residues Lys505-Ala591) more than 30% of identical residues. Thus 3kas.pdb template was also used for modeling the RNF13 C-terminal domain (Figure 2).

PTM predictions. The NetPhos 3.1 server was used for predicting phosphorylation at serine, threonine or tyrosine of the full-length sequences of RNF13 wild type and variant-containing

sequences. Both generic and kinase specific predictions are performed. NetPhos3.1 performs make for the following 17 kinases: ATM, CKI, CKII, DNAPK, EGFR, GSK3, INSR, PKA, PKB, PKC, PKG, RSK, SRC, cdc2, cdk5 and p38MAPK, CaM-II.

Supplemental references

1. van Schadewijk A, van't Wout EF, Stolk J, Hiemstra PS (2012) A quantitative method for detection of spliced X-box binding protein-1 (XBP1) mRNA as a measure of endoplasmic reticulum (ER) stress**.** Cell Stress Chaperones. 17, 275-279

2. Pierri, C., Parisi, G., Porcelli, V. (2010). Computational approaches for protein function prediction: A combined strategy from multiple sequence alignment to molecular docking-based virtual screening. Biochim Biophys Acta, 1804, 1695-1712

3. Larsson, P., Wallner, B., Lindahl, E., Elofsson, A. (2008). Using multiple templates to improve quality of homology models in automated homology modeling. Protein Sci. 17, 990-1002.

4. Sánchez, R., Sali, A. (2000) Comparative protein structure modeling. Introduction and practical examples with modeller. Methods Mol Biol, 143, 97-129

5. Barlow, P.N., Luisi, B., Milner, A., Elliott, M. (1994). Everett R. Structure of the C3HC4 domain by 1H-nuclear magnetic resonance spectroscopy. A new structural class of zinc-finger. J Mol Biol 237, 201-211.

6. Abraham, J., Corbett, K.D., Farzan, M., Choe, H., Harrison, S.C. (2010). Structural basis for receptor recognition by New World hemorrhagic fever arenaviruses. Nat Struct Mol Biol 17, 438-444.

7. Lobley, A., Sadowski, M., Jones, D. (2009) pGenTHREADER and pDomTHREADER: new methods for improved protein fold recognition and superfamily discrimination. Bioinformatics, 25, 1761-1767.

8. Webb, B. Sali, A. (2014). Protein structure modeling with MODELLER. Methods Mol Biol 1137, 1-15.